BACKSCATTERING INTERFEROMETRY AS A DIAGNOSTIC TOOL

By

Carolyn Sue Enders

Thesis

Submitted to the Faculty of the

Graduate School of Vanderbilt University

in partial fulfillment of the requirements for

the degree of

MASTER OF SCIENCE

in

Chemistry

December, 2009

Nashville, Tennessee

Approved:

Professor Darryl J. Bornhop

Professor Charles M. Lukehart

ACKNOWLEDGEMENTS

I am sincerely grateful for the financial support of Vanderbilt University which provided the means to complete these studies. It has been a true honor to interact with the distinguished scientific community here at Vanderbilt University, and I can envision no better environment in which to flourish as a young scientist. In particular, I am indebted to my advisor, Dr. Darryl Bornhop, for his support and guidance not only as the principle investigator in these studies but also as a mentor to me in my graduate career. I am grateful to have been influenced by Dr. Bornhop's intelligence, creativity, and determination which mark him as a true leader in scientific advancement.

I would also like to thank each member of the Bornhop lab for helping to create a supportive and collaborative environment in which we all assist one another to achieve research goals. I truly understand and appreciate how unique such an environment is. In particular, I would like to acknowledge the guidance of Amanda Kussrow, an incredibly meticulous and intelligent fellow graduate student who was always willing to assist me and others, even while immersed in a significant amount of work herself.

Finally, this thesis would not have been possible without the support and encouragement of my family. I am particularly grateful that my parents taught me at a very early age to challenge myself and to continually explore the farthest reaches of my intellect and capabilities. I am also honored to have found an incredibly dedicated fellow chemist and a role model in my husband Jeffrey Enders. I truly would not be the researcher I am today without the support, insight, and assistance he has provided me every single day of my graduate career.

TABLE OF CONTENTS

LIST OF FIGURES

Figure

CHAPTER I

INTRODUCTION TO INTERFEROMETRY

Applications of Interferometry across the Disciplines

When two or more light waves are superimposed, an interference pattern is created. By studying these patterns, the properties of the light waves and of the material that they have been in contact with can be explored. This field, known as interferometry, has led to the development of some of the most sensitive optical techniques available and has been applied to various applications, including astronomy, metrology, oceanography, seismology, and biological sciences.

Interferometry was first applied in the field of astronomy over two centuries ago to investigate why stars appear larger through a telescope relative to other objects.[1] Later, the technique was utilized to determine the actual diameter of various astronomical objects.[2, 3] Today, astronomical interferometers have provided some of the highest resolution images of our galaxy.[3] In the field of applied metrology, interferometry is an essential tool used to characterize optical components; for example, the technique may be used to detect deformations in mirror blanks or to inspect the quality of a lens or an optical fiber.[4-6] In oceanography, interferometry has been used for imaging ocean surface features, such as currents and wave movements.[7, 8] Seismology frequently utilizes interferometry to image the topography of the earth, and can be used to measure and study deformations caused by events such as earthquakes and explosions.[9, 10]

Interferometric Biosensors

Interferometry has also been applied to biological sciences as a tool to monitor and quantify molecular interactions. Within this field, interferometry offers the dual advantage of being a highly sensitive technique that does not require the use of expensive molecular labels. Therefore, molecular interactions may be characterized with both binding partners in their native states, eliciting quantitative, meaningful (i.e. unperturbed by labeling) affinity data in a cost-effective format. Here we explore several different types of interferometers which have been successfully utilized to study molecular interactions.

Mach-Zehnder interferometer

The Mach-Zehnder interferometer (MZI) utilizes a waveguiding method to monitor the difference in refractive index (RI) between a sample and reference arm of the waveguide (Figure 1.1). A laser illuminates a single-mode waveguide which is then split into a sample and reference arm. The reference arm is coated with a thin cladding layer, while the sample arm has a window to allow the evanescent field to interact with the sample. The sensor and reference arms are then recombined, leading to beam interference. Any change in the sample's refractive index produces a phase shift in the sensor arm beam, which in turn results in a change in the output intensity when the two beams are recombined. Binding events are thereby measurable using photodetection. Intrinsically, the evanescent sensing approach of the MZI instrumental configuration requires a single polarization and single-mode illumination to prevent interference from cross-polarization and multimodal effects. The sensitivity of the MZI is typically

correlated with the length of the sensing window, making it difficult to measure low concentrations of analytes without using large amounts of sample.

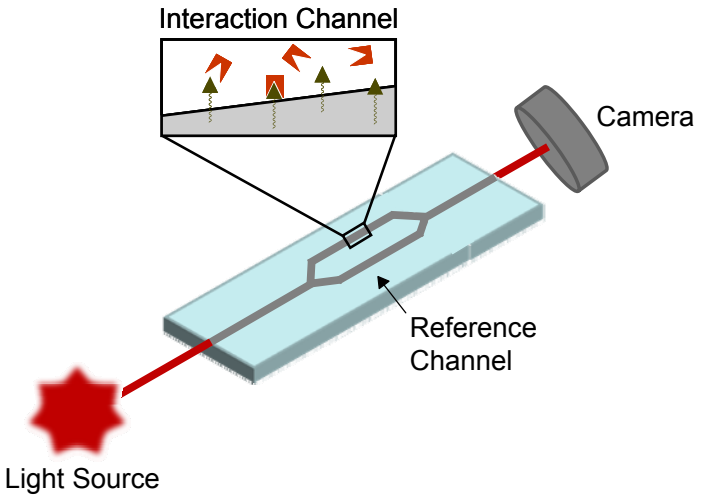

Figure 1.1 Illustration of a Mach-Zehnder interferometer

The MZI was first used for biosensing in 1993 and has since been utilized in a broad range of applications.[11-15] In 1997, Brosinger et al. demonstrated the ability to resolve a refractive index change of 2×10^{-5} refractive index units (RIU) with their early MZI configuration.[12] Initial experiments to test the biosensing ability of the instrument were also reported, demonstrating that MZI can detect fetal calf serum binding nonspecifically to the sensor surface.[12] More recently, Prieto et al. used a Mach-Zehnder interferometer total internal reflection (MZI-TIR) configuration to achieve a minimum refractive index change of 7×10^{-6} at the sensor surface. The utility of the instrument was demonstrated by detecting the interaction between a covalently immobilized pesticide and its antibody in PBST (phosphate buffered saline Tween).[13] The same group also constructed an MZI based on a rib anti-resonant reflecting optical waveguide

(ARROW). The use of ARROW structures instead of conventional TIR waveguides allows for larger core and rib dimensions, making the instrument more compatible with mass-production and also lowering insertion losses. However, these advantages are accompanied by a loss in sensitivity -- the minimum detectable refractive index change for the MZI-ARROW was found to be 2×10^{-5}.[14]

Young interferometer

Another waveguiding interferometer is the Young interferometer (YI). The YI configuration includes a single-mode laser illuminating a single-mode waveguide, which is then split into a sample and reference arm, as in the Mach-Zehnder interferometer. However, instead of the interference being created when the waveguides recombine as in the MZI, in a YI the optical output of the waveguides interact in free space to create the interference fringes, which are displayed onto a CCD camera (Figure 1.2).

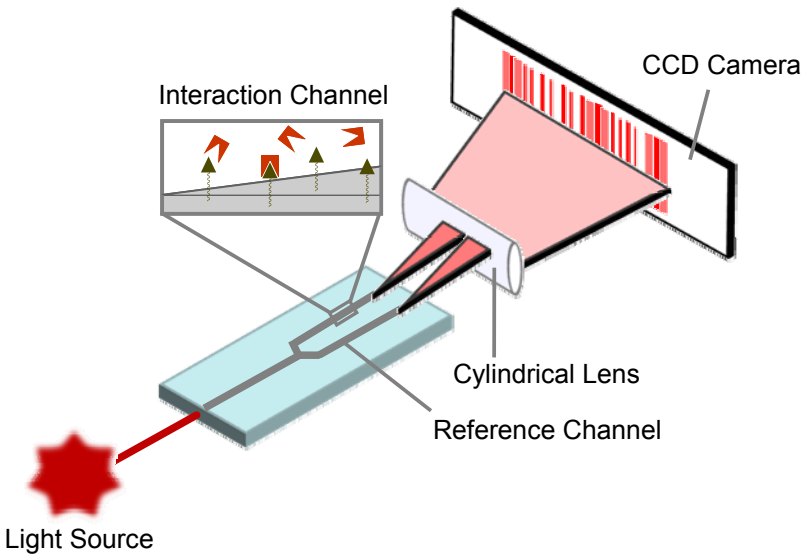

Figure 1.2 Illustration of a Young interferometer

The YI was first used to measure molecular interactions in 1994[11] and has been widely published on thereafter.[16-18] In 2003, Ymeti et al. showed that their multi-channel YI configuration can measure four different analyte concentrations simultaneously, achieving a refractive index resolution of 8.5×10^{-8} RIU.[16] In 2006, Hradetzky et al. reported a refractive index detection limit of 0.9×10^{-6} for their single-cell YI, and detected the hybridization of 21-mer DNA with immobilized receptor DNA at the biosensor surface.[17] Their findings suggested the detection limit of this DNA-DNA binding interaction to be in the picomolar range.

Hartman interferometer

The Hartman interferometer (HI) is also a waveguiding technique; however, in contrast with the MZI and YI, this approach utilizes a planar waveguide that is patterned with lines of immobilized molecules (Figure 1.3). Light is directed into the waveguide through a grating to create a single broad beam. The light then passes through parallel sensing regions which are coated with different receptors to create distinct binding and control regions. The light then travels though integrated optics that combine the light from neighboring regions to create interference. The interference signals then pass through another grating and to the detector. The phase shift of the interference patterns is measured to detect refractive index changes.

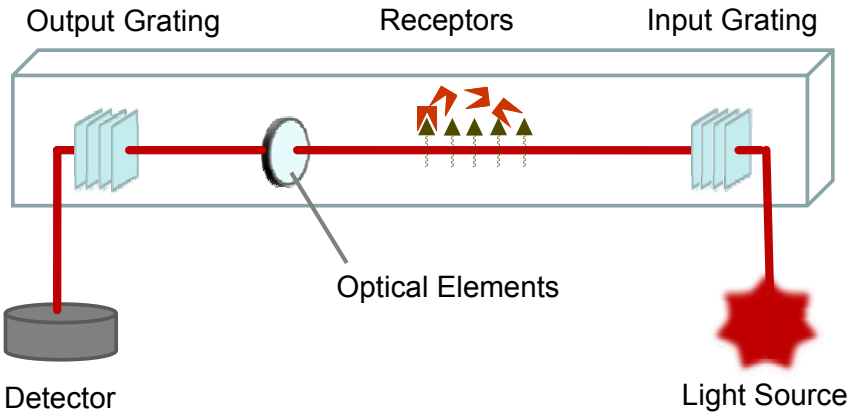

Figure 1.3 Illustration of a Hartman interferometer

In 1997, Schneider et al. demonstrated the broad applications of the HI as a real-time detector of nucleic acid, protein, and pathogen analytes. Experiments were performed by immobilizing the receptor (anti-hCG antibody) to the sensor surface, allowing for real-time detection of human chorionic gonadotropin (hCG) with a direct detection limit of 2 ng/mL in phosphate buffered saline (PBS). DNA hybridization experiments detected a four-base mismatch in 50% formamide hybridization buffer, and a nucleic acid detection capability of 10^{11} copies per mL was achieved.[19] In early 2000, the same group expanded on these applications, demonstrating the ability of their configuration to detect hCG in human serum at clinically relevant levels of 0.1 ng/mL. Extensive studies of the nonspecific binding associated with serum samples were also performed, which concluded that the HI can overcome this particular setback using a reference region and controlled surface chemistry.[20] Later that year, Schneider et al. took their studies a step further by detecting hCG in whole blood; despite significantly higher background levels than buffer or serum systems, a clinically relevant detection limit of 0.5 ng/mL hCG was achieved.[21]

Diffraction optics

Diffraction-based sensing employs a similar technique of immobilizing the probe molecules into a pattern that will diffract the incoming laser light to create an interference pattern (Figure 1.4). This pattern has been shown to change as sample is introduced and binding occurs on the stripes of capture species, resulting in a change in the height and refractive index of the diffraction grating. The intensity of the refractive spots is measured using a photodectector, allowing any changes within the sample to be measured. While many applications of diffraction optics offer enhanced performance when used in conjunction with labeling strategies, the following examples focus primarily on label-free applications of the technique.

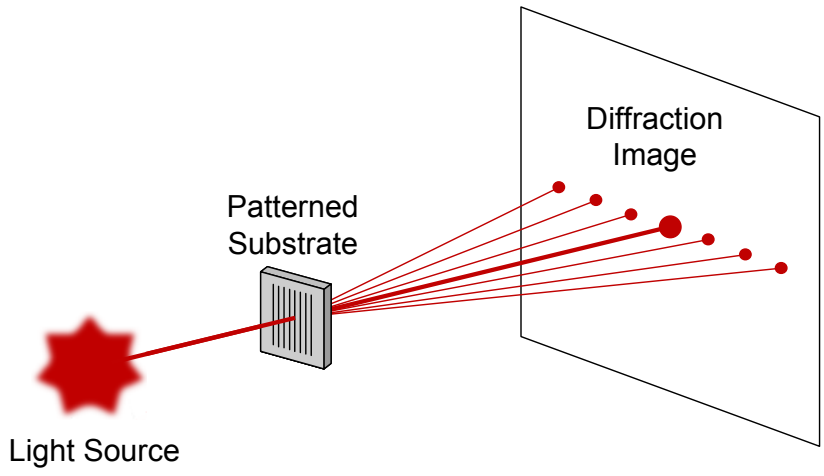

Figure 1.4 Illustration of a biosensor based on diffraction optics

Early studies by St. John et al. demonstrated that diffraction optics can be used to detect whole bacteria cells captured using an antibody grating stamped on a silicon surface.[22] In 2005, Goh et al. demonstrated the ability of diffraction optics to measure

two different binding interactions simultaneously without the use of labels. To achieve this, receptor molecules mouse IgG and rabbit IgG were immobilized in two different patterns via PDMS stamping on the same 2D surface. Anti-mouse IgG and anti-rabbit IgG were then introduced into the cell sequentially. The binding observed for each pattern indicated the specific binding of the target analyte exclusively to its receptor antibody. These findings carry implications for diagnostic applications involving multiple markers and/or competition assays.[23] Currently, Axela Biosensors offers a commercialized diffraction-based sensor known as the dotLab™ System which enables multiplexing of immunoassays over a broad dynamic range. In 2007, they demonstrated the ability to simultaneously measure binding of two similar sets of antibody/analyte pairs with concentrations which differed by 6 orders of magnitude; however, labeling strategies were implemented to measure the analyte of lower concentration.[24]

Dual polarization interferometer

The dual polarization interferometer (DPI) is another waveguide method for studying molecular interactions. This technique utilizes two waveguides, a sample and reference waveguide, which are stacked together, so they may be illuminated by a single laser (Figure 1.5). The light exiting the waveguides form an interference pattern in the farfield. In contrast with other waveguide sensors, the polarization of the laser in the DPI is alternated so that two polarization modes of the waveguides are excited in succession in order to modulate the signal and increase sensitivity. Using the information from the measurements of both polarization states, the refractive index and the thickness of the adsorbed protein layer can be calculated.

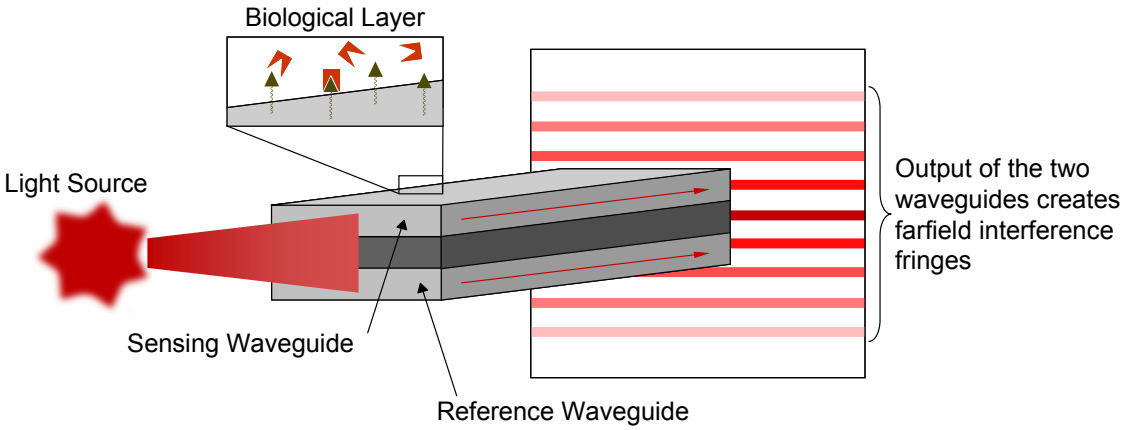

Figure 1.5 Illustration of a biosensor based on dual polarization interferometry

In 2003, Swann et al. measured the binding and surface loading of streptavidin to the biotin-functionlized surface of their DPI. Nonspecific binding, thickness and density changes of protein layers as well as other structural aspects of the streptavidin-biotin system were also explored in detail using this tool.[25] In 2006, Lin et al. used DPI to derive dissociation constants (K_D) for homopolyvalent pentameric C-reactive protein (CRP) with monoclonal anti-CRP IgG; these values were in close agreement with those previously derived using enzyme-linked immunosorbent assays (ELISA).[26] That same year, Ricard-Blum et al. measured the interaction of immobilized heparin with heparin binding protein HepV. Exploring the stochiometric and kinetic parameters of this binding system using DPI lent insight into collagen V interaction with proteoglycans in tissues, a process which affects collagen fibril formation.[27] In 2009, Wang et al. utilized DPI to measure the structural changes of electrostatically immobilized DNA upon binding to small molecules ethidium bromide and spermine in real time. Changes in mass, thickness, and refractive index of the DNA sample layer (consisting of either native

or denatured DNA) were monitored upon small molecule binding. These studies harnessed the ability of DPI to measure structure and kinetics simultaneously and the flexibility of the technology to interrogate binding interactions over a large molecular size range.[28] Farfield Sensors, Ltd has been commercializing DPI-based biosensing systems since 2000 with the introduction of the AnaLight® 250, and has most recently released the AnaLight® 4D which enables the measurement of structural changes within lipid bilayers.[27, 29, 30]

Porous Si sensors

Porous silicon sensors have been developed using the principles of the Fabry-Perot interferometer on thin films of porous silicon etched in a silicon substrate. The porous Si film acts as the interferometer, creating fringes from reflections off the top and bottom of the pores (Figure 1.6). As demonstrated by Sailor, et al. in 1999, this technique can overcome typical penetration depth limitations because the entire volume of the sample within the film is utilized for the measurement.[31, 32] Limited penetration depth, or the inability to measure interactions which occur above the sensor surface, is a significant shortcoming present in other surface-based techniques.

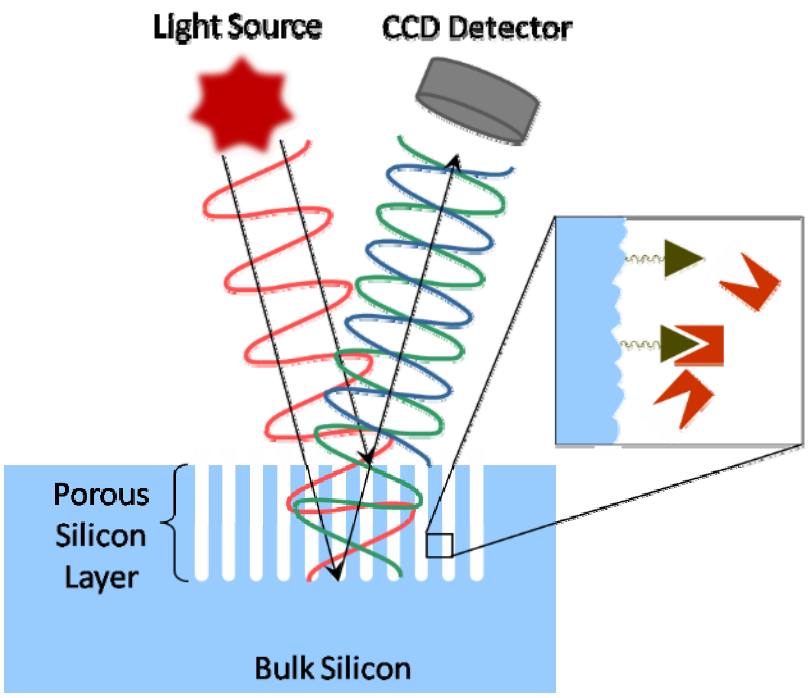

Figure 1.6 Illustration of a Porous Si sensor

A 1997 *Science* paper by Lin, et al. reported the ability of a porous silicon-based optical interferometric bionsensor to detect the binding of small molecules, DNA oligomers, and proteins with unprecedented sensitivity (pico- and femtomolar concentrations).[31] In 1999, Dancil et al. studied protein A and IgG binding via porous silicon biosensing. This report highlighted the reversibility and stability of the system, as well as the ability to render the sensor insensitive to nonspecific binding.[32] A 2003 publication in *Science* by Li et al. demonstrated that porous silicon can serve as a template for the construction of complex optical structures (comprised of organic polymers or biopolymers, e.g.) in biosensor applications. These more recent findings are of particular interest to drug delivery applications.[33]

BioCD

The biological compact disk (BioCD) utilizes patterns of immobilized capture proteins on a disk with a mirrored surface to create periodic reflective interference spectra which are measurably altered by binding (Figure 1.7).[34, 35] The interference signal is interrogated before and after the disk has been incubated with the sample, and the difference is correlated to the amount of binding that has occurred. Unfortunately, because the BioCD discretely measures the relative difference in the reflectance patterns of surface immobilized proteins before and after binding, the tool is not readily applicable for real-time monitoring, rendering kinetics studies problematic.

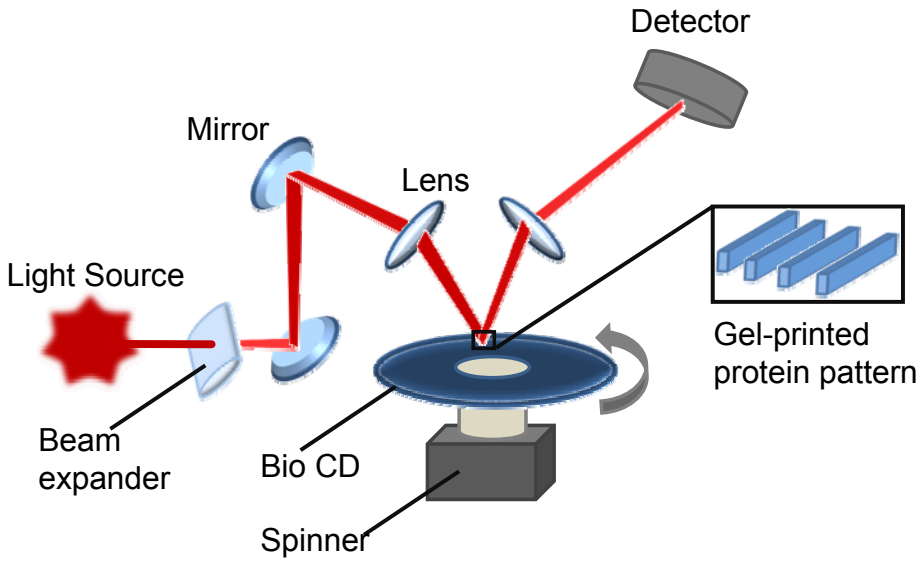

Figure 1.7 Illustration of a BioCD

Detection limits as low as 10^5 molecules has been achieved using the BioCD, which was employed to measure specific binding between anti-mouse IgG and mouse IgG using rabbit IgG as a control.[34, 35] In an expanded effort, it was shown that binding

measurements are concentration-dependent, illustrating the potential of the technique for quantitative analyses.[36] In 2009, Wang et al. expanded applications of the technique further by employing the BioCD to perform multiplexed prostate specific antigen (PSA) detection in human serum.[37]

Other reflective interferometric platforms

Recently, the principles of reflectance interferometry used in porous silicon and BioCD methods have been applied to other biosensor variations with increased multiplexing abilities. In particular, Ozkumer et al. have introduced a multiplex platform known as the spectral reflectance imaging biosensor (SRIB) designed for high throughput use. SRIB is based on the optical phase difference rendered by the binding of biological species to probes on a transparent layered surface. This technique enables the collection of reflectance spectra for hundreds of spots on the array simultaneously.[38, 39] Gauglitz et al. have used reflective interferometric spectroscopy (RIfS), a similar platform based on multiple white light reflections at thin transduction layers, to characterize biomolecule interactions in a multiplexed, high throughput format by attaching 96- and 384-well plates to the transducer slide.[40] The varied applications of this RIfS platform include use a screening tool for thrombin inhibitors and antibodies against triazine libraries.[40, 41] Biametrics is currently developing a commercial version of the RIfS platform.[42, 43]

Backscattering interferometry

A new technique, backscattering interferometry (BSI), was originally used to measure small refractive index changes in fused-silica capillaries.[44] and has been developed in multiple configurations and for a wide array of applications.[45-51] BSI has

more recently been employed to study molecular interactions in a label-free method and has proven to be a versatile sensing technique; BSI can be used to investigate binding events in both a surface-immobilized scheme and in free solution. This ability to measure interactions in a free-solution format makes BSI unique among interferometric techniques. The free-solution advantage not only eliminates the time and monetary costs related to immobilization strategies, but also allows binding partners to be monitored entirely in their native state. Furthermore, because BSI is dually amenable to both free-solution and surface-immobilized formats, any contribution of immobilization to binding perturbation may be measured directly. Perhaps surprising in light of the platform's versatility is that BSI consists of an extremely simple optical train, requiring only a collimated coherent light source, a capillary or microfluidic chip (hemispherical or rectangular), and a detector.

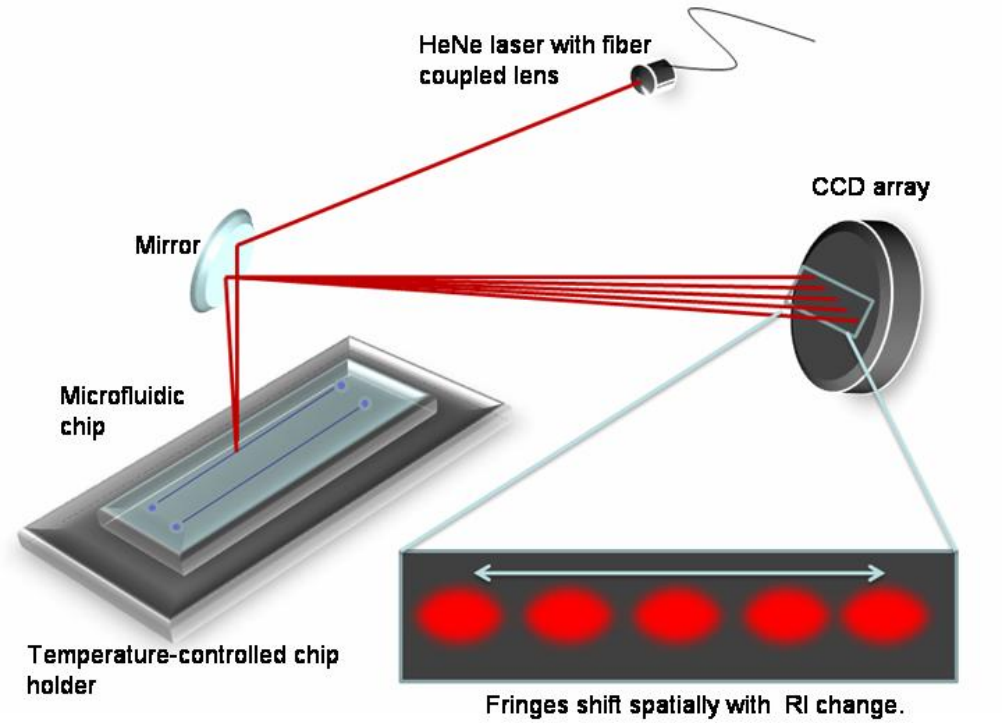

Figure 1.8 Illustration of a backscattering interferometer

In the latest configuration of BSI, a microfluidic chip molded in polydimethylsulfoxide (PDMS) or etched in glass is employed. BSI utilizes a red helium-neon (HeNe) laser (λ = 632.8 nm) to illuminate the microfluidic channel (Figure 1.8). While not absolutely necessary, the laser may be coupled to a collimating lens through a single-mode fiber. When the laser beam impinges the channel and interacts with the fluid contained within the channel, a set of high contrast interference fringes is produced and monitored in the direct backscatter region at relatively shallow angles. The spatial position of these fringes depends upon the refractive index (RI) of the fluid within the channel. The change in fringe position is monitored using a CCD array in combination with Fourier analysis, enabling the quantification of the shift as a change in

spatial phase, calculated in the Fourier domain.[52] Molecular interaction studies performed in recent years using BSI technology will be detailed in Chapter II.

CHAPTER II

BACKSCATTERING INTERFEROMETRY AS A BIOSENSING TOOL

Background and Significance

Current label-free biosensing techniques for measuring protein interactions include surface plasmon resonance (SPR), calorimetric methods such as isothermal titration calorimetry (ITC), and interferometric methods such as backscattering interferometry (BSI).[53] SPR measures refractive index changes near a gold surface to detect binding. Although widely-used, SPR requires surface immobilization of targets and uses expensive gold-plated sensor chips of limited reusability.[53-55] ITC measures reaction enthalpy to detect label-free binding events, but large sample volumes are typically required. Furthermore, sensitivity is diminished by low or zero-value reaction enthalpies.[56] As discussed in Chapter I, among the many interferometric biosensing techniques available, BSI is unique in its ability to interrogate label-free molecular interactions in either a heterogeneous (surface-immobilized) or a homogeneous (free-solution) format at picomolar levels using picoliter volumes (corresponding to 10,000's of molecules measured).[56] Furthermore, in comparison with other label-free techniques such as SPR and ITC, BSI provides unmatched sensitivity and is the only tool that is fully compatible with microfluidics.[53]

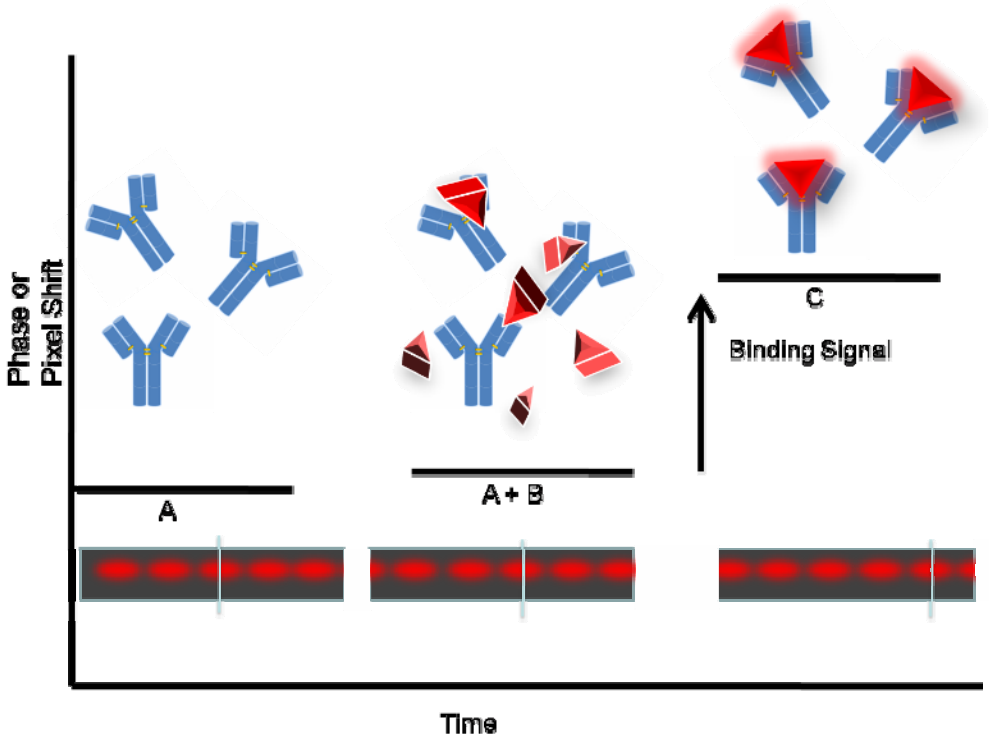

Figure 2.1 Illustration of a binding event and the subsequent BSI signal produced.

Heterogeneous Assays

Originally BSI facilitated interaction assays in the heterogeneous mode, utilizing the immobilization of one binding partner onto the surface of a microfluidic chip molded in polydimethylsiloxane (PDMS).[53, 54] In early experiments, streptavadin was immobilized onto the channel surface and the fringe pattern was measured before and after introducing biotin into the channel. A good correlation was found between the BSI molecular interaction signal and the fluorescence signal reported in a similar experiment. Next, a biotinylated protein-A (P_A) surface allowed the monitoring of reversible IgG-P_A interactions with femtomole detection limits.[35] New surface chemistry enabled a two-fold improvement on detection limits of the protein A-IgG interaction without the use of a fluorescent label, and also allowed monitoring of the hybridization of complimentary

strain of DNA at concentrations ranging from 5nM to 500 mM to a 30-mer of mActin. Assuming 100% surface coverage, the 3σ limit of quantification was found to be 36 attomoles of DNA in the 500 pL detection volume. Further experiments showed that a 3 base pair mismatch could be detected, evidenced by a marked decrease in binding signal from that of the original complimentary strand – only 7 % of the signal generated by the binding of the complimentary strands was observed for the mismatched strand.[54]

The extraordinary sensitivity of BSI was further demonstrated by expanding on these preliminary observations to study lectin-sugar binding.[57] Since BSI is not a film thickness sensor (i.e., signal is not dependent on a change in mass at the sensor surface), it was possible to measure the binding of concanavilin A (con A) to mannose and glucose and the binding of a lectin isolated from *Griffonia simplicifolia* (BS-1) to galactose. Biotinylated lectins (proteins) were attached in functional form to the surface of glass microfluidic channels coated with extravidin by simple mixing.[58] The binding of unmodified carbohydrates was monitored by BSI and dose-response curves were used to generate values for association constants. Mannose and glucose were found to bind to the lectin concanavalin A with dissociation constants of 42 ± 5 μM and 155 ± 88 μM, respectively; galactose bound to BS-1 lectin with a dissociation constant of 30.2 ± 2.8 μM.[57] This study is significant because it demonstrates that BSI uniquely allows quantification of a binding event for just *one part in 1000 change in mass*, allowing the protein to be tethered and the small molecule to be titrated. To our knowledge this small molecule - protein assay has never been performed in this manner on another platform and represents a challenging assay for widely-used label-free techniques.

In order to study multivalent interactions, the carbohydrate studies were then expanded to measure the binding of sugar-coated virus particles (cowpea mosaic virus (CPMV) and bacteriophage Qβ virus-like particles).[57] CPMV particles with approximately 200 mannose molecules attached to the surface with three different linkers and were studied. The binding of these virus particles to immobilized Con A was monitored and the saturation binding isotherms were plotted to determine the association constants. Comparison of the affinity of the particles to that of free mannose showed an average of a 100-fold increase in affinity on a per-glycan basis. Similarly, two different Qβ particles (450 and 470 mannose per particle) were studied, and the K_D values showed an approximately 220 fold increase in affinity over that of free mannose on a per glycan basis.[57] These studies illustrate that BSI has the potential to measure polymeric binding and the effects of cooperation.

Free-Solution Assays

Likely the most novel aspect of BSI is that it can be used to measure free-solution molecular interactions. Using a channel with a serpentine mixer and a restriction to mix the two interacting species on-chip, a stop-flow experiment can be performed label-free and in free solution to elicit real-time kinetic data. Using these methods, systems reported were Protein A (P_A) which binds with high affinity to the F_C region of several immunoglobulin G (IgG) species, including human and rabbit; calmodulin (CaM), the ubiquitous calcium-binding protein that can bind to and regulate a multitude of different protein targets; and the interaction between IL-2 and a monoclonal antibody, in this case in buffer and in cell-free media. Recent advancements of BSI have shown that molecular

interaction assays can be performed utilizing exceedingly small amounts of sample at physiologically relevant concentrations, without the use of labels or surface immobilization, and in complex matrices. For example, the entire CaM study (i.e., CaM-Ca^{2+}, CaM-TFP, CaM-M13 peptide, and CaM-calcineurin) required the consumption of only about 200 picomoles or 3 mg of CaM, and each binding event only required one minute for analysis.[56]

By quantifying the picomolar binding affinity of IL-2 in cell-free media,[56] it was demonstrated that BSI has the potential to evaluate high-affinity interactions and is compatible with matrices more complex than buffer. This unique ability to study free-solution binding in complex matrices sets BSI apart.

Recently published results indicate that BSI can be used to screen structurally destabilized mutants of the T4 lysozyme (T4L) against the small heat-shock protein (sHSP) α-crystallin.[59] sHSPs constitute a superfamily of molecular chaperone proteins, which help other proteins to fold properly to prevent aggregation. Molecular chaperones have been linked to cataracts and neurodegenerative diseases such as Alzheimer's and Parkinson's.[59-61] In these experiments, the differential binding of chaperone proteins to T4L mutants of varying stabilities was quantified, demonstrating the remarkable specificity of BSI in characterizing binding interactions.[59]

Although each of these examples were performed using a mixer chip to facilitate online mixing of reagents, it should be noted that solutions may also be pre-mixed off chip, enabling the determination of affinity measurements using an end-point format.[56]

CHAPTER III

BSI AND DIAGNOSTIC APPLICATIONS USING SYPHILIS AND HIV AS MODELS

BSI as an Attractive Diagnostic Tool

The ability of BSI to measure interactions rapidly using picoliter detection volumes in a free-solution format makes BSI unique among sensing techniques, eliminating time and monetary costs related to labeling and immobilization strategies. BSI will now be applied to disease-detection methods with the potential application as a reactive serum detector. In collaboration with the Centers for Disease Control and Prevention (CDC) in Atlanta, GA, syphilis and human immunodeficiency virus (HIV) serology will be used as models for evaluating the diagnostic performance of BSI.

Current diagnostic tools rely heavily on signaling moieties to detect the presence of a particular antigen or antibody in a sample. Such chemical labeling not only consumes time and resources, but may also alter the conformations and/or behavior of binding partners, obscuring test results.[62] Introducing this variable necessitates that many common label-based diagnostic assays must be corroborated by additional testing methods, further increasing time, cost, and sample consumption.[63] Diagnostics for diseases with a heavy worldwide presence and with marked prevalence in developing areas, such as syphilis and HIV, are particularly sensitive to time, cost, and sample volume considerations. Therefore, a label-free microfluidic diagnostic tool has the potential to revolutionize point-of-care diagnostics for these and other widespread diseases.

Of the available label-free techniques, BSI provides unmatched sensitivity and is the only tool that is fully compatible with microfluidics – critical advantages for diagnostic applications.[56] BSI's ability to detect antigen-antibody interactions has previously been established by the Bornhop group.[56] In order to explore BSI's capacity to detect syphilis and HIV infections in human sera, purified antigens will be used to detect antibodies in the sera raised against the infection. Successful detection of syphilis and HIV infections in human specimens using BSI will not only provide innovative diagnostic approaches for these particular infections, but will serve as a benchmark in protein-based diagnostics, applicable to countless other diseases. Using BSI to detect antigen-antibody interactions decreases cost, time, and sample volume considerations and may also offer the unique potential to quantify antibody levels in clinical samples. Such an advantage may provide valuable information concerning disease status, severity, progression, and/or therapeutic efficacy.

Syphilis Serology

Background and Significance

Syphilis is a sexually-transmitted infectious disease caused by the bacterium *Treponema pallidum* for which no adequate in vitro culturing method has been developed.[64, 65] Therefore, current syphilis diagnostic tests typically rely on the detection of anti-treponemal antibodies raised against the pathogen itself (i.e., treponemal tests) as well as nontreponemal tests for antibodies against lipoidal material released from damaged host cells and against lipoprotein-like secretions of the treponeme.[64, 65] The

most commonly used treponemal tests include the fluorescent treponemal antibody absorption (FTA-ABS) and the treponemal pallidum particle agglutination test (TP-PA), and current nontreponemal tests include the Venereal Disease Research Laboratory (VDRL) and the Rapid Plasma Reagin (RPR) tests.[64, 65] While treponemal tests are highly specific, they give little or no indication of the status of the infection because anti-treponemal antibodies are retained for a lifetime. In contrast, nontreponemal tests are most reactive during active syphilis infection; when the disease is latent or has been effectively treated, the reactivity of the antiserum to these tests subsides.[9] However, nontreponemal tests have shown a high rate of false-positive results (i.e., are relatively nonspecific) because anti-cardiolipin antibodies may be generated as a result of conditions unrelated to syphilis, including autoimmune diseases, tuberculosis, pregnancy, and vaccinations.[66] Therefore, it is most informative to perform a treponemal and a nontreponemal diagnostic test in concert; a typical clinical diagnosis may be based upon an RPR or VDRL screening followed by a TP-PA or FTA-ABS confirmation.[65]

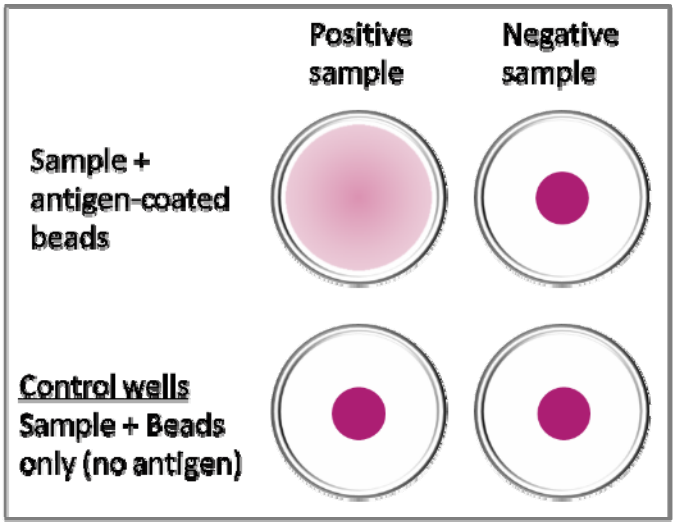

Figure 3.1 Illustration of TP-PA test well-plate. Reactive (i.e. "positive") samples spread across the bottom of the well as the serum antibodies agglutinate with the antigen-coated beads.

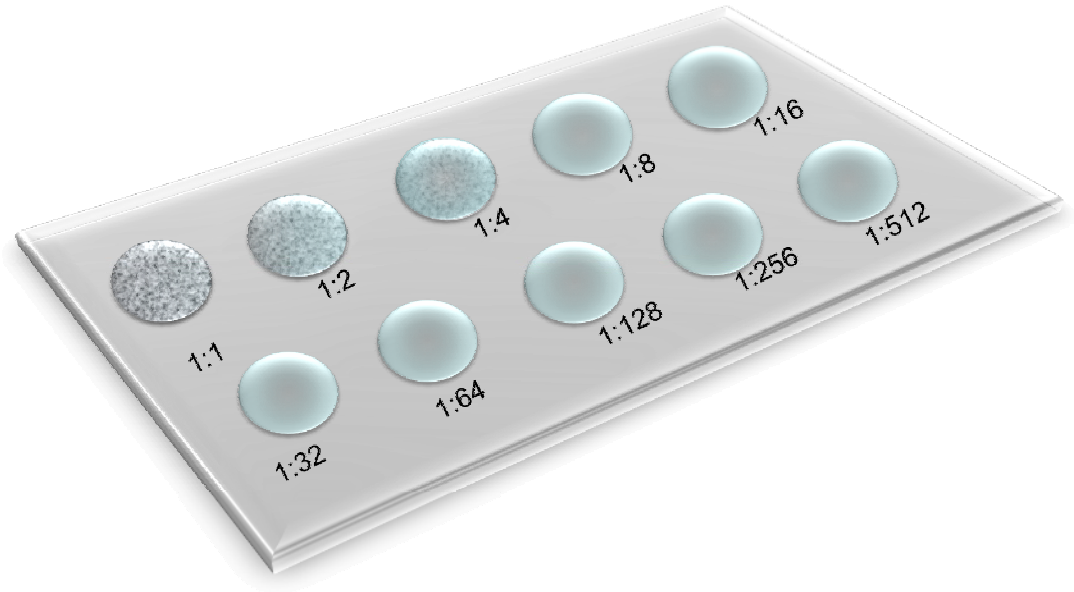

Figure 3.2 Illustration of RPR test card. The reactivity of this sample would be characterized as "R4" due to inadequate antibody-antigen clumping of subsequent dilutions.

Each of these diagnostic tests relies on a visual interpretation of results and/or labeling. The FTA-ABS utilizes the reaction of fluorescently-labeled anti-IgG antibodies

with anti-treponemal serum antibodies bound to an antigen-coated slide, detected using fluorescent microscopy. The TP-PA test employs antigen-coated colored gelatin particles to visualize the hemagglutination of reactive antiserum (Figure 3.1). The VDRL test evaluates the level of clumping between antiserum and a nontreponemal antigen containing cardiolipin, lecithin, and cholesterol as seen under a visisble light microscope.[64, 65] The RPR test utilizes charcoal as a visualizing agent to detect this same clumping reaction with the naked eye (Figure 3.2). The application of BSI to syphilis diagnostics would enable both treponemal and nontreponemal tests to be performed rapidly in a single low-volume assay format without the use of fluorescent tags, visualizing agents, or microscopy, decreasing time and cost considerations and increasing the quantitative potential of nontreponemal tests.

Experimental procedures

Small aliquots from fractions number 2 – 6 of affinity-purified total IgG from a rabbit inoculated with the syphilis-causing bacterium *Treponema pallidum* were obtained from the CDC. Increasing concentrations of total IgG (using fraction #5) were prepared in phosphate buffered saline (PBS), and each concentration was mixed with either a recombinant treponemal antigen r17 (Genway Biotech, Inc.), a nontreponemal free cardiolipin antigen (Sigma-Aldrich), or PBS to serve as a calibration. The final concentrations of the total IgG were 0 – 50 μg/mL and the final antigen concentration was held in excess at 100 μg/mL. The BSI signal was measured for each sample, and the bulk contributions of IgG and antigen were subtracted from the binding measurements

using the IgG calibration. The remaining signal, representing the antigen-antibody binding, was plotted versus IgG concentration.

Serum-based experiments paralleling the treponemal syphilis binding assay in buffer were conducted using a nonreactive (negative control) commercial serum sample obtained from a TrepSure enzyme immuno assay kit (Phoenix Bio-Tech Corporation) mixed with the increasing concentrations of total IgG (prepared using fraction #4). Each concentration was then mixed with either recombinant treponemal antigen r17 antigen or PBS. The final mixtures contained a 1:40 dilution of serum and an r17 antigen concentration of 100 μg/mL with IgG concentrations ranging from 0 to 50 μg/mL. The BSI signal was measured for each sample and the bulk contributions of IgG, serum, and r17 antigen were subtracted in order to obtain the signal created during the binding event. This signal was plotted versus total IgG concentration.

Clinical serum samples from human patients used for syphilis serology experiments were provided by the CDC, having been previously classified according to reactivity using the treponemal particle agglutination (TP-PA) test and the nontreponemal rapid plasma regain (RPR) test. The serum samples were first diluted with PBS and were then mixed with either A) a recombinant treponemal antigen r17 (resulting in a final concentration of 5 ug/mL r17) or B) a micellar cardiolipin antigen (resulting in a final dilution of 1:800 micelle prep). It should be noted that this micellar cardiolipin antigen is a synthetic antigen newly developed by the CDC to enhance the specificity of cardiolipin-based assays, and therefore precise concentration information was not available. Binding measurements were performed on-site at the CDC using a commercial BSI instrument that, while possibly more sensitive, is also more prone to chip clogging

than the configuration used in previous experiments; therefore, final serum dilutions were increased to 1:400. The binding signal of the interaction was measured and plotted versus the serum classification.

Results and Discussion

Results from BSI assays measuring syphilis antibody – antigen interactions in PBS are shown in Figure 3.3. This data indicates that the binding of the total immunoglobulin G (IgG) from a syphilitic rabbit to both treponemal and nontreponemal antigens produces a BSI signal. Furthermore, this signal correlates with the quantity of IgG in the sample, assuming that an excess of antigen (recognized only by specific anti-treponemal IgG) is present. It should be noted that because this IgG preparation consists of total IgG and is not limited to specific anti-treponemal IgG molecules, the IgG concentrations noted here are arbitrary in that the actual concentration of IgG potentially binding to the antigen in these samples is unknown. Therefore no affinity information regarding the interaction may be extracted.

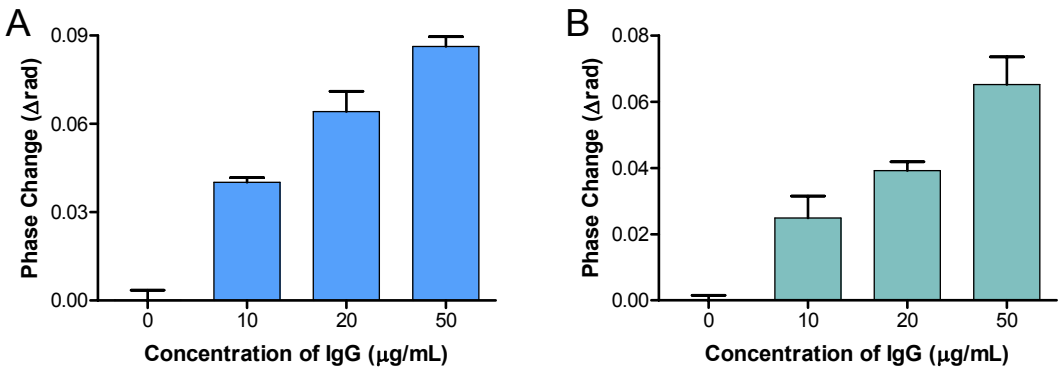

Figure 3.3 BSI signal resulting from the reaction of purified total IgG in buffer with A) 100 ug/mL r17 antigen and B) 100 ug/mL free cardiolipin antigen. Error bars represent the standard deviation of triplicate determinations.

The binding of the treponemal antigen with the IgG in the presence of human serum is shown in Figure 3.4. These results indicate that this reaction (and presumably other antigen-antibody reactions) may be detected against the complex serum matrix. Notably, a significantly lower signal is observed for the binding of each IgG concentration in serum than for the corresponding measurement performed in buffer. This muted signal suggests that a lower number of specific binding interactions are being detected above the calibration signal. This apparent decrease in specific binding interactions may be the result of nonspecific binding between serum proteins and IgG in both the calibration and the binding assays, lowering the effective IgG concentration in the assay. Alternatively, because these two measurement were performed using different IgG fractions (though both from the same extraction collected from a single animal), the quantities of specific anti-r17 IgG may differ for corresponding total IgG concentrations.

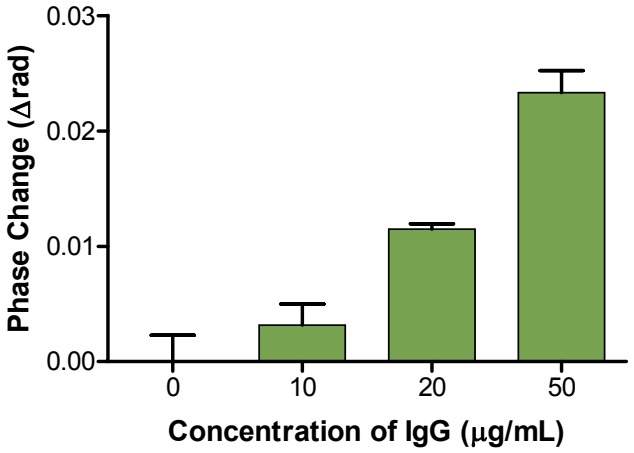

Figure 3.4 BSI signal resulting from the reaction of total IgG with 100 ug/mL r17 in the presence of human serum. Error bars represent the standard deviation of triplicate determinations.

To expand on these studies, preliminary experiments to explore the potential performance of BSI as a reactive serum detector were performed using clinical human serum samples from syphilitic and healthy individuals. The BSI signal indicating the binding interaction of treponemal r17 antigen with each of 20 human serum samples, pre-classified according to syphilis infection status and RPR titer strength, is shown in Figure 3.5(A). Titer strength is determined according to the highest serum dilution which still displays adequate clumping in the presence of the antigen in the RPR test; higher dilutions imply higher reactivity.[64] However, because the RPR test utilizes a nontreponemal cardiolipin antigen and measures the level of cardiolipin antibodies in the serum, an RPR titer may, but is not necessarily expected to, correlate with signals generated using a treponemal antigen. Therefore, the element of interest for this nontreponemal assay is the separation of positive from negative samples and not their correlation with titer strength. Indeed, Figure 3.5(B) shows a statistically significant

separation ($p=1x10^{-5}$) between BSI signals for positive and negative samples, demonstrating that a signal threshold may be established for determining the reactivity of unclassified samples. These results show promise for the application of BSI as a reactive serum detector.

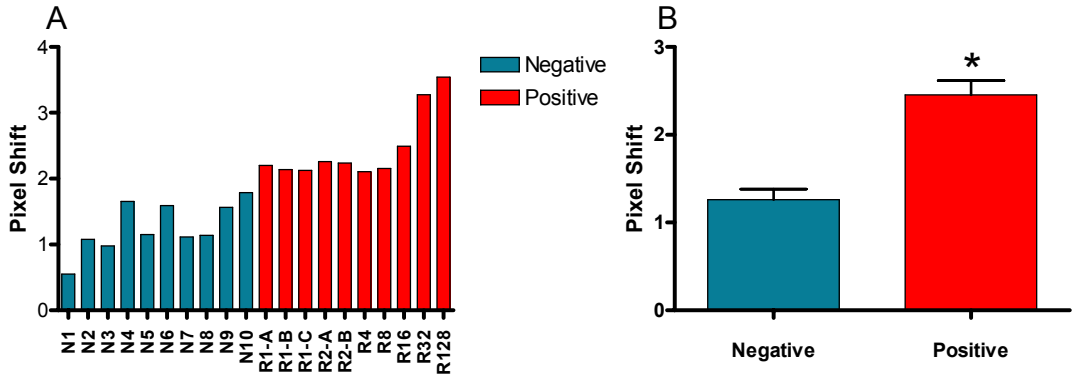

Figure 3.5 A) BSI signal resulting from the reaction of human serum samples (pre-classified according to titer strength with regard to syphilis infection) with r17 antigen. **B)** Average of signals for positive and negative samples (error bars represent the standard deviation of 10 samples), showing a statistically relevant separation between positive and negative signals (*$p=1x10^{-5}$).

Figure 3.6 shows the resultant BSI signal from the reaction of a micellar cardiolipin antigen with 20 human serum of various titer strengths, according to the syphilis RPR test. Figure 3.6.A demonstrates a correlation between the RPR titer strength and the measured BSI signal for nearly every sample. This result is expected since a nontreponemal cardiolipin antigen is used in both the BSI determinations and the RPR test (i.ei, both assays aim to quantify serum antibodies raised specifically against cardiolipin antigens). Further studies would be necessary to determine the reasoning for the anomalous reading of R1-A, which gives a BSI signal markedly larger than the other two samples with R1 titer strength.

Figure 3.6.B shows a statistically significant separation ($p=5x10^{-6}$) between BSI signals for positive and negative samples. These results demonstrate that that a signal threshold may be established for determining the reactivity of unclassified samples using a cardiolipin antigen, as was demonstrated with the treponemal antigen in figure 3.5.B.

Overall, the the assay results shown in Figures 3.5 and 3.6 not only reiterate the potential of BSI to be used not as a reactive serum detector, but also show that BSI may enable the quantification of antibody levels in patient samples. Perhaps most importantly, the ability to achieve congruent BSI results using two markedly different antigen probes highlights the multiplexing possibilities of BSI to streamline diagnostic approaches.

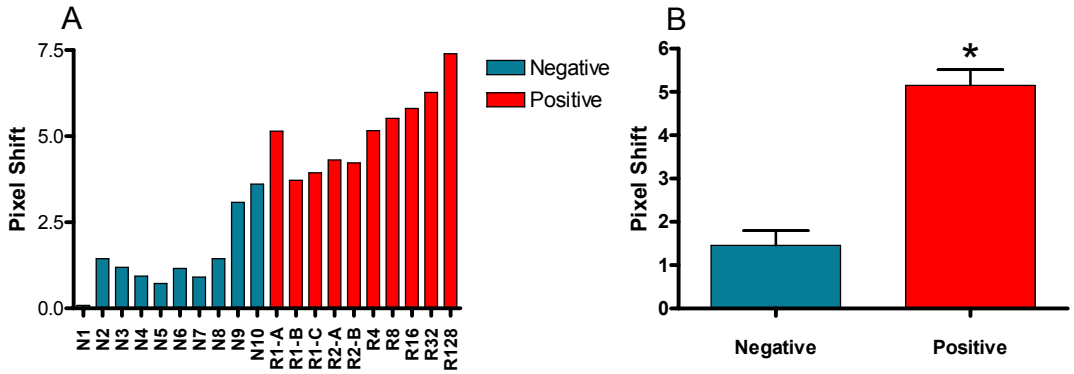

Figure 3.6 A) BSI signal resulting from the binding of human serum samples (pre-classified according to titer strength with regard to syphilis infection) with micellar cardiolipin antigen, showing a correlation between RPR titer strength and BSI signal. **B)** Average of signals for positive and negative samples (error bars represent the standard deviation of 10 samples), showing a statistically relevant separation between positive and negative signals ($p=5x10^{-6}$).

HIV Serology

Background and Significance

Human immunodeficiency virus (HIV) is a retrovirus which causes acquired immunodeficiency syndrome (AIDS), a pandemic life-threatening disease that severely compromises the immune system of infected individuals. Routine HIV diagnostics test for serum antibodies raised against HIV proteins using the enzyme-linked immunosorbant assay (ELISA).[67-69] If a positive result is obtained with this initial screening, a second diagnostic test is typically performed using a different assay format, such as a Western blot or an immunofluorescence assay (IFA), to confirm the result.[67, 69]

Each of these methods requires labeling strategies for the visualization of serum antibodies. Illustrated in Figure 3.7, an ELISA test used for HIV diagnostics typically involves the addition of patient serum to wells containing immobilized HIV antigens (inner core protein p24, envelope protein gp41, and envelope protein gp120, e.g.). Ideally, only specific antibodies against these proteins remain in the wells following stringent wash procedures. Bound antibodies are then detected using a secondary anti-human antibody conjugated to an enzyme such as horse-radish peroxidase, a common labeling enzyme which produces a visual signal following the addition of a substrate.[68, 69] A Western blot also involves the incubation of patient anti-serum with viral proteins, and the resultant complexes are separated from other serum proteins using gel electrophoresis. Protein bands are then transferred to a nitrocellulose or polymer sheet where they are visualized using radiolabeled antibodies.[69] IFA employs a similar strategy, using whole T cells which have been infected with HIV to react with serum

antibodies rather than protein antigens. Any antibodies bound to the infected T cells are visualized using a fluorescently-labeled secondary anti-human antibody.[69] As discussed previously, eliminating the need for costly and disruptive labeling strategies in any diagnostic approach is ideal, thus highlighting the benefit of applying BSI detection strategies to HIV and other diseases.

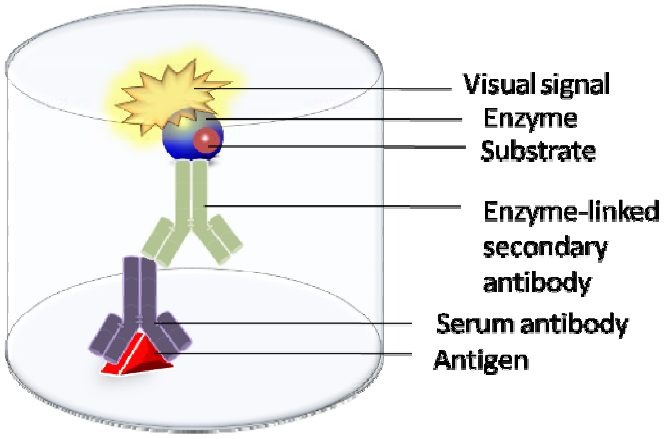

Figure 3.7 Illustration of the ELISA (indirect) method for detecting specific antibodies.

Like syphilis serology, HIV diagnostics would also benefit from the quantitative potential of BSI. In the early stages of HIV infection, high concentrations of viral core protein p24 are secreted and anti-p24 antibodies appear. The presence of this core protein and its antibody response therefore serve as the earliest serological indicators of HIV infection. Levels of this antigen and, subsequently, its antibody, decrease as the disease progresses.[68] Because of this phenomenon, the quantification of p24 is currently being explored as an early detection and/or prognostic tool for HIV infection. Furthermore, the measurement of viral load through serological p24 quantification shows promise as an effective yet less expensive, less time-consuming, and less labor-intensive

approach than HIV-RNA quantification, the current standard technique for determining HIV viral load.[70, 71] Utilizing BSI to perform a p24-based diagnostic assay may not only offer enhanced sensitivity for both early disease detection and quantification of viral load, but may also minimize time, cost, and labor investments associated with these measurements.

Experimental procedures

Affinity-purified, anti-p24 monoclonal IgG antibody (MAb) was obtained from the CDC. Increasing concentrations of anti-p24 MAb were prepared in PBS, and each concentration was mixed with a fixed concentration of p24 antigen, also received directly from the CDC, or with PBS to serve as a calibration. The final concentrations of the anti-p24 MAb were 0 – 800 nM, and the final p24 antigen concentration was held constant at 1 nM. The BSI signal was measured for each sample, and the bulk contributions of the MAb were subtracted using the MAb calibration. The remaining signal, representing the antigen-antibody binding, was plotted versus MAb concentration to form a saturation isotherm. The K_D value for this binding system was then determined using Prism™ software by fitting to a single-site binding model using a square hyperbolic function.

Clinical serum samples from human patients used for HIV serology experiments were provided by the CDC, having been previously classified as positive or negative using standard commercial testing methods, such as ELISA. Serum samples were first diluted with 0.1% BSA in PBS and were then mixed with a recombinant protein containing the immunodominant gp41 transmembrane regions for 3 subtypes of HIV-1 class M (denoted rIDRm), developed by the CDC. Sera samples were reacted with

antigens to a final sera concentration of 1:20 and a final antigen concentration of 4.75 μg/mL. For each sample, a control was prepared which consisted of the sera diluted 1:20 in buffer with no antigen present. The change in signal, or phase shift, was measured between each control serum and the reacted sample (containing the same serum plus antigen).

Results and Discussion

An endpoint saturation binding curve constructed using BSI measurements to evaluate the affinity of p24 for the CDC-developed anti-p24 MAb is shown in Figure 3.8. From the saturation isotherm plot, the K_D for this antigen-antibody pair is calculated to be 77.1 nM ± 16.7 nM ($R^2 = 0.99$). Notably, no affinity information was previously known for this binding system due to the fact that the antibody was newly synthesized and was thus far uncharacterized, highlighting the distinct advantage that BSI can be used to make novel K_D determinations. Results suggest that the new MAb does indeed bind with the p24 antigen with nanomolar affinity. Comparing these results with BSI data collected for other anti-p24 antibodies may serve as a screening approach for predicting the relative performance of these synthetic antibodies in diagnostic assays for HIV.

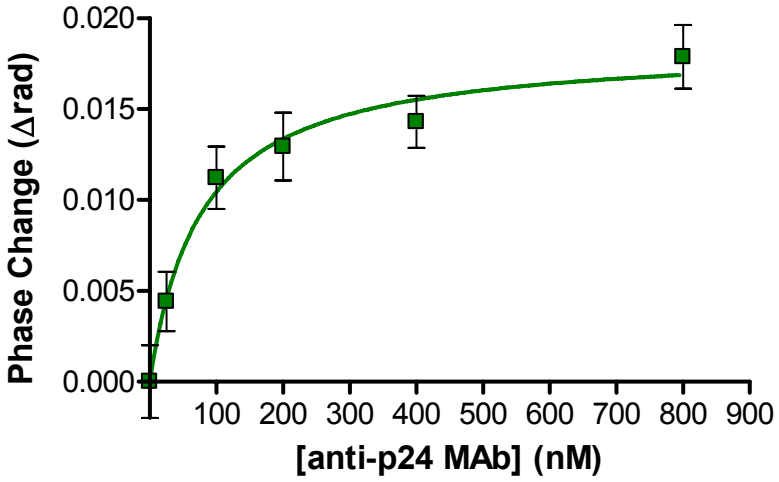

Figure 3.8 BSI signal resulting from the reaction of purified p24 with purified recombinant anti-p24 MAb. Error bars represent the standard deviation of the noise in the measurement.

The reaction of human serum samples, pre-classified according to HIV infection status, with newly received rIDRm antigen yielded positive changes for positive samples and negative changes for negative samples (Figure 3.9). These results suggest that a bulk negative change in the refractive index of the sera is observed in response to the addition of the rIDRm antigen, but a positive RI change is observed if binding occurs. Although very few samples were analyzed and the assay has not yet been optimized, these preliminary results show promise for BSI as a reactive serum detector for HIV and other diseases.

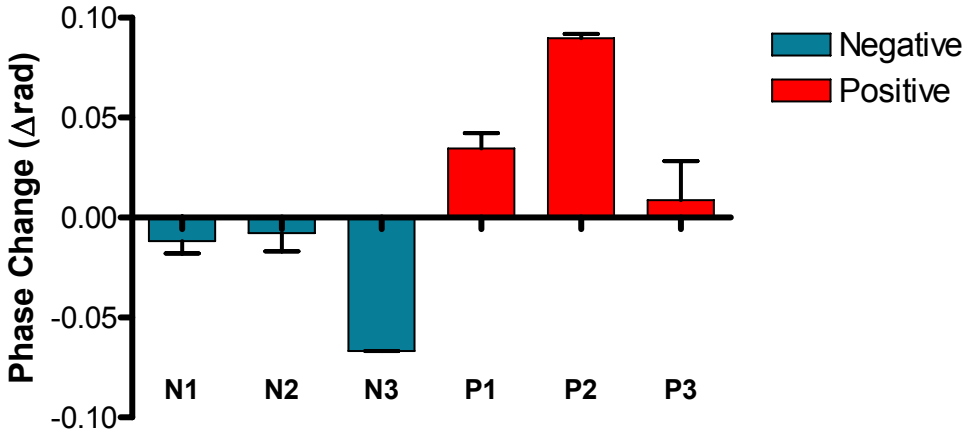

Figure 3.9 BSI signal resulting from the reaction of human serum samples (pre-classified as positive or negative with regard to HIV infection) with rIDRm antigen. Error bars represent the standard deviation of two trials.

Conclusions

The experiments performed using human serum samples demonstrate that BSI may be capable of serving as a reactive serum detector in a clinical setting. Primarily, a clear threshold between reactive and nonreactive sera may be determinable for a panel of samples using both treponemal and nontreponemal antigens. Furthermore, the BSI signal arising from the binding of antiserum and nontreponemal micellar cardiolipin antigen shows a strong correlation with the semi-quantitative RPR test currently in practice. Preliminary results of assays interrogating rIDRm reaction with human serum samples also show that reactive and nonreactive sera may be distinguished using BSI. These results show promise for utilizing BSI to perform rapid serological tests using a variety of molecular probes, offering many possibilities for multiplexed, possibly quantitative assays to improve current clinical diagnostics. Furthermore, BSI may enable the characterization and evaluation (i.e., screening) of novel biosensing molecules, such as

the anti-p24 MAb developed by the CDC, to aid in the development of more specific and sensitive diagnostic approaches applicable to virtually any assay format.

CHAPTER IV

BSI CONFORMATIONAL STUDIES USING REOVIRUS AS A MODEL

Background and Significance

BSI and conformational changes

The precise source of the unique binding signal measurable using BSI in free-solution is currently under investigation. Because real-time BSI measurements of binding signals are observed to level off following equilibrium, the signal must result from permanent changes in the refractive index of the interrogated medium, eliminating thermal changes as a dominating source of the signal. [56] Furthermore, BSI has demonstrated the ability to readily detect the binding of the calcium ion (Ca^{2+}) to calmodulin (CaM), a 16 kDa protein, in real-time. Because of the significant discrepancy in size between these two binding species, changes in mass are also insufficient to explain the signal source. However, upon binding with Ca^{2+}, CaM undergoes a marked conformational change during which many waters of hydration (>35/CaM) are ejected from the compound.[72] The ability to monitor this phenomenon has helped to illuminate the role of structural and/or molecular dipole changes in producing a signal detectable using BSI. We therefore hypothesize that the BSI signal results from structural changes and effects on the molecular dipole of the medium resulting from the interaction of binding species. Such changes probably involve the folding or unfolding of molecules and/or changes in waters of hydration upon binding.[56].

Here we aim to further explore the ability of BSI to interrogate conformational changes within a molecular system, even in the absence of binding. Specifically, we will measure signal differences between reovirus in its native state and following disassembly induced by acid exposure and/or proteolytic activity. These experiments will lend insight into BSI's ability to harness induced conformational changes in molecules as a possible diagnostic or signaling strategy. For example, if two different virus particles generate different BSI signal profiles when exposed to the same protease, it may be possible to utilize these unique profiles in a diagnostic strategy. Another potential utility of this phenomenon would be to use molecules which are known to undergo characteristic structural changes upon exposure to a particular chemical as a signaling moiety. These molecules could be attached to a targeting antibody, potentially enhancing the binding signal between the antibody and its target when conformational changes are induced.

Reovirus Disassembly

Reovirus is a non-enveloped double-stranded RNA virus which can be isolated from human respiratory and enteric tracts but is not associated with significant disease in humans.[73, 74] However, reovirus has been widely studied as a model for understanding the cellular proteolysis of viral proteins, a process which has been implicated in the mechanism of infection for influenza virus, rotavirus, HIV, and others.[75] Furthermore, reovirus has recently shown promise as a novel therapy for the treatment of cancer due to its preferential replication in some cancerous cells; phase II clinical studies are currently underway.[73, 74, 76]

Reovirus is comprised of an outer capsid of viral proteins surrounding the "core," or inner capsid, which is a multienzyme complex providing the components necessary for viral replication.[75, 77] Upon infection of a cell, outer capsid proteins undergo dramatic structural changes. Specifically, the virion first attaches to the cell via outer capsid protein σ1, initializing uptake by the cell into acidic compartments known as endosomes (i.e., receptor-mediated endocytosis).[75, 78] This acidic environment, in combination with acid-dependent endosomal proteases, is believed to facilitate the conversion of the reovirus from a virion to an intermediate subviral particle (ISVP).[75] Once inside the cytosol of the cell, the ISVP undergoes further disassembly into the core particle and replication occurs. As shown in Figure 4.1, an ISVP particle lacks the outer coat of σ3, an extended form of σ1 is present, and outer capsid proteins μ1 and μ1C (designated μ1/C in Figure 4.1) are converted to δ and φ peptides. In conversion to the core particle, σ1, δ, and φ are lost completely[75].

In collaboration with the Chappell and Dermody labs at Vanderbilt University, the intracellular disassembly of reovirus will be studied as a model for A) measuring conformational changes using BSI and B) better understanding the viral and host determinants that regulate proteolysis in reovirus, which may also be applicable to other infectious viruses. Specifically, the ability of BSI to monitor reovirus conversion from virion to ISVP to core particle will be studied using *in vitro* strategies for generating these reovirus products, such as digestion using chymotrypsin or titration with acid. While the *in vitro* digest of reovirus by chymotrypsin is a well-established method for facilitating conversion to ISVP and core particles, mimicking the *in vivo* activity of acid-dependent proteases cathepsin B and cathepsin L, it is less certain whether a low pH

alone will induce significant conformational changes in the virion.[76, 78, 79] If BSI enables the successful detection and quantification of conformational changes associated with the reovirus disassembly process, this novel biosensing strategy will then be used to assess differences in the kinetics of outer-capsid proteolysis between different reovirus mutants. These studies will not only lend insight into the physical origins of the BSI signal, enabling us to harness conformational changes to design any number of diagnostic assays, but may also contribute to an advanced understanding of uncoating processes in viral infection.

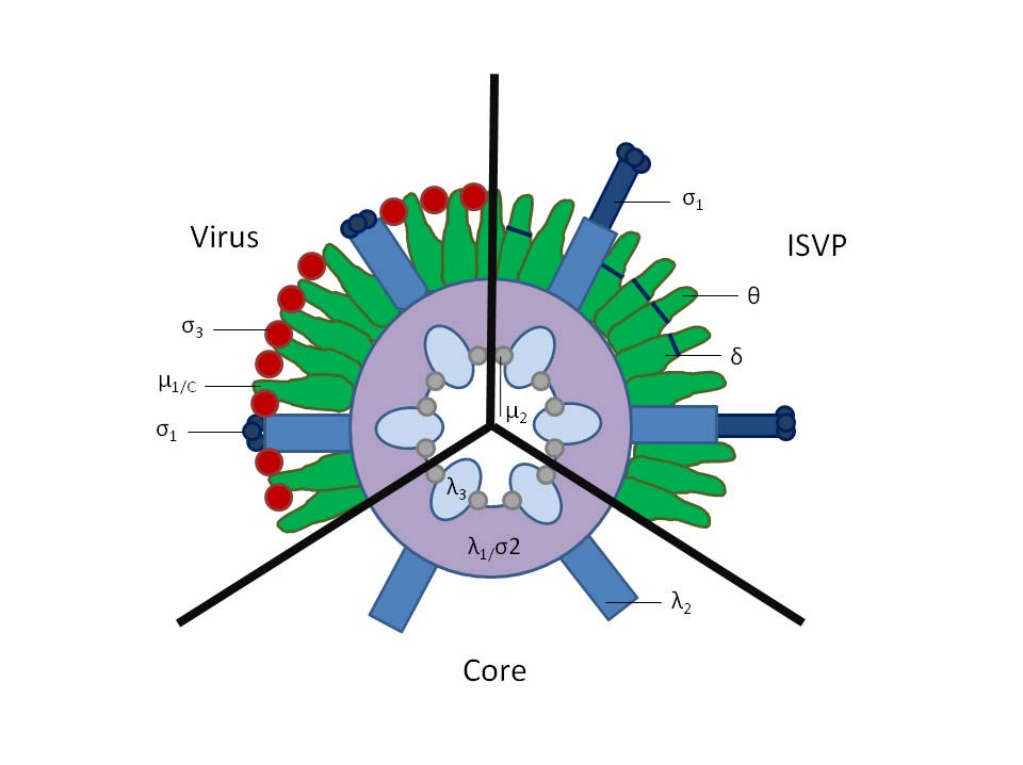

Figure 4.1 Illustration of reovirus as a virion, ISVP, and core particle

Experimental Procedures

Acid titration of dialysis buffer

A Tris-based buffer (dialysis buffer) was prepared (150 mM NaCl, 15 mM $MgCl_2$, 10 mM Tris, pH 7.4). A fixed volume of increasing concentrations of hydrochloric acid (HCl) was added to aliquots of dialysis buffer to achieve final HCl concentrations of 0 – 4 mM. The pH of each sample was then measured and plotted versus HCl concentration.

Acid titration of Reovirus

Purified virions of reovirus type 1 Lang (T1L), dialyzed into a Tris-based buffer (150 mM NaCl, 15 mM $MgCl_2$, 10 mM Tris, pH 7.4), were obtained from the Chappell laboratory. T1L was diluted to a concentration of 1.2×10^9 particles/mL using dialysis buffer and aliquoted. A fixed volume of increasing concentrations of HCl was added to these aliquots to achieve final HCl concentrations of 0 – 4 mM. Samples were allowed to react for 20 minutes, followed by measurement of the BSI signal for each acid concentration point. Corresponding acid concentrations in dialysis buffer alone were also prepared and the BSI signal was measured to serve as a calibration. The bulk contribution of acid was subtracted from the T1L titration measurements using the calibration curve, and the resultant BSI signal (due to conformational changes of the virions) was plotted versus acid concentration.

Chymotrypsin digest of Reovirus

Aliquots containing equivalent concentrations of T1L in Tris-based dialysis buffer were exposed to Nα-Tosyl-Lys-chloromethylketone (TLCK)-treated chymotrypsin (Sigma-Aldrich) for A) 1 hour, and B) 2 hours at 37^{o}C. At the appropriate time point, the reaction was stopped with the enzyme inhibitor phenylmethanesulphonylfluoride (PMSF). Final reagent concentrations were 2 x 10^{12} particles/mL T1L, 200 μg/mL chymotrypsin, and 2 mM PMSF. The BSI signal was measured for each time point immediately following the addition of PMSF. A solution of 2 x 10^{12} particles/mL T1L alone (replacing chymotrypsin and PMSF with equivalent volumes of dialysis buffer) was also prepared to serve as the "0 hour" time point. In addition, solutions of 200 μg/mL chymotrypsin and 2 mM PMSF were prepared and the BSI signal was measured to determine the bulk refractive index contributions of these reagents. Bulk contributions of PMSF and chymotrypsin were subtracted from the T1L digest measurements at 1 and 2 hours. The resultant BSI signal (due solely to conformational changes of the virions) was zeroed according to the bulk signal of the "0 hour" sample (representing no conformational change) and was plotted.

SDS-PAGE analysis of digest results

Sodium dodecyl sulfate polyacrylamide gel electrophoresis (SDS-PAGE) was performed on products generated via chymotrypsin digest of reovirus. Specifically, 4 x 10^{10} viral particles of each sample were dissolved in 6X SDS sample buffer (0.35 M Tris, pH 6.8, 30% glycerol, 10% SDS, 0.6 M dithiothreitol). Samples were heated to 98^{o}C for 5 minutes and loaded onto a 4-20% gradient Tris-HCl gel (Bio-Rad). Proteins were

resolved by electrophoresis in Laemmli buffer (0.025 M Tris, 0.2 M Glycine, 0.1% SDS) at a constant voltage of 120V for 1.5 hours. The gel was fixed and stained using colloidal blue (Invitrogen) and visualized using and Odyssey infra-red imager (Li-Cor.)

Results and Discussion

Figure 4.2 shows the pH values for a range of acid concentrations in dialysis buffer. These experiments were performed to determine the acid concentration yielding the desired pH range to mimic the endosomal environment in this particular buffer system, providing insight into the approximate acid concentration where conformational changes may be expected to begin when titrating reovirus with HCl. Based on these results and the assumption that reovirus disassembly occurs in endosomes (pH range of 5-6), conformational changes (if occurring at all) would be expected to be induced at acid concentrations above 2 mM HCl in dialysis buffer.

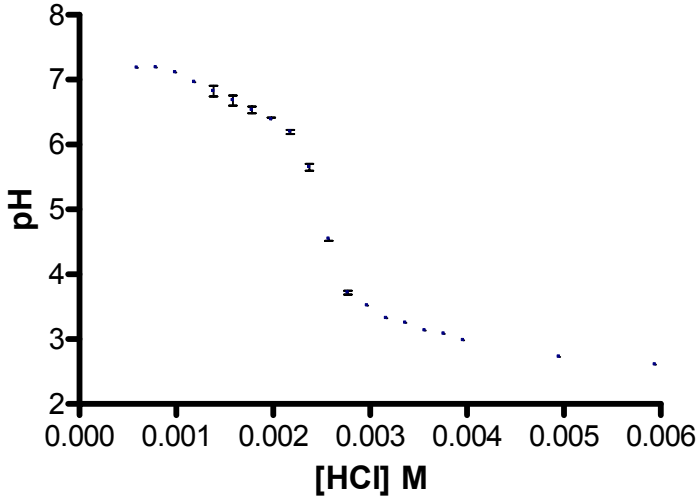

Figure 4.2 pH values for the various acid concentrations (final) in dialysis buffer. Error bars represent the standard deviation of triplicate determinations.

The results of the acid titration of reovirus T1L strain at a concentration of 1.2 x 10^9 particles/mL are shown in Figure 4.3. Although the measurements are very noisy (error bars represent 3 trials of both the acid calibration curve and the T1L titration), a sharp downward signal is observed at an acid concentration of approximately 2.2 mM, corresponding to a pH of approximately 6.15. Notably, a negative signal is not unexpected as conformational changes may result in either a positive or negative change in refractive index. Although these preliminary results suggest that reovirus may be undergoing conformational changes in the presence of acid at concentrations resembling those of endosomes, more studies must be performed to confirm the relevance of this data. In particular, this assay may benefit greatly from an increase in reovirus concentration and/or an increase in incubation time, supported by the observation that the exposure of 2 x 10^{12} reovirus particles/mL to chymotrypsin for 1-2 hours produces a distinguishable but not excessively large signal in Figure 4.4.A. Presumably, any conformational changes owed to pH alone would be less significant than those induced by protease digestion. Therefore, the concentration of T1L necessary to observe acid-induced changes in conformation is likely to be greater than or equal to that necessary to observe protease-induced conformational changes.

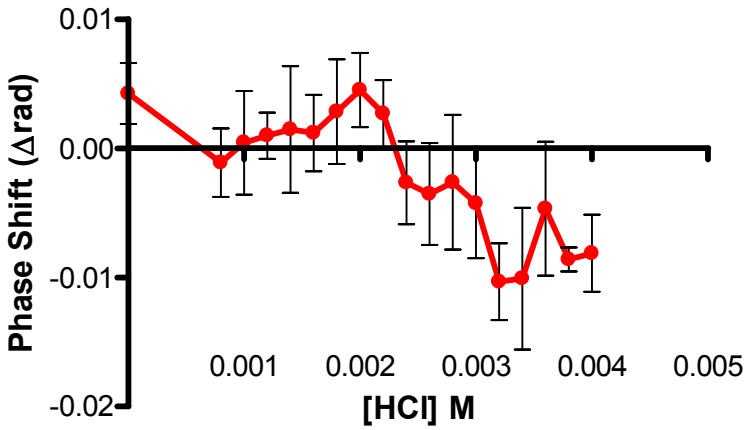

Figure 4.3 BSI signal resulting from the reaction of reovirus T1L strain (1.2×10^9 particles/mL) with acid at various concentrations. Error bars represent the combined standard deviations of 3 trials of both the acid calibration curve and the T1L titration.

The results of the chymotrypsin digest of T1L are shown in Figure 4.4.A. Reovirus concentration was increased to 2×10^{12} reovirus particles/mL in order to provide sufficient product for protein visualization on an SDS-PAGE gel Figure 4.4.B. These results demonstrate that a negative BSI signal results from T1L disassembly, an observation that corroborates the suspicion that acid titration may initiate degradation (a negative trend, albeit far less pronounced, is also seen in Figure 4.3). A marked change in BSI signal is observed upon reovirus exposure to chymotrypsin for 1 hour, and this signal continues to increase in magnitude as supported by what is seen on gel. Gel results taken of these same samples following digestion indicate that after a 1 hour exposure to chymotrypsin, most of the T1L particles have converted from the virion stage to the ISVP stage. This conversion is evidenced by the near disappearance of μ1 and σ3, and the appearance of δ (see figure 4.1 for structural significance of these bands). While the aim of the 2-hour exposure to chymotrypsin was to achieve conversion from ISVP to core particle, the gel results show that this additional change did not occur. However, the

further disappearance of μ1, the complete disappearance of σ3, and the appearance of a more prominent δ band show that the majority of virions remaining after the 1 hour digestion were converted to ISVPs after 2 hours. Therefore, the observation that the BSI signal change from 1 to 2 hours is clear, yet less dramatic than the signal change from 0 to 1 hour, is not surprising.

Although further studies must be performed to understand how the BSI signal might change if the conversion from ISVP to core particle is achieved, it is suspected that the signal may plummet markedly as observed for the conversion of virion to ISVP. Specifically, Coombs suggests that a 3-hour chymotrypsin digest using the same assay conditions may achieve the full conversion of virion to core particle.[77] Furthermore, a wealth of information may be gained from a *real-time* analysis of T1L digestion over the course of several hours. Such an experiment may assist in more precisely identifying the BSI signal change resulting from individual protein alterations of T1L during disassembly by enabling the construction of a real-time kinetics profile of these reactions.

Once BSI profiles for the proteolytic conversion of the T1L wild-type to its ISVP and core particle stages are well-established, other strains, such as Type-3 Dearing (T3D), and mutants of these strains will be interrogated in the same manner and compared to T1L wild-type. Specifically, the Dermody lab studies reovirus mutants which demonstrate differences in the time course of proteolytic conversion. These experiments will not only investigate the ability of BSI to distinguish pathogens based on differences in induced conformational changes, but may also lend insight into the kinetics of viral capsid proteolysis for these different reovirus mutants and strains.

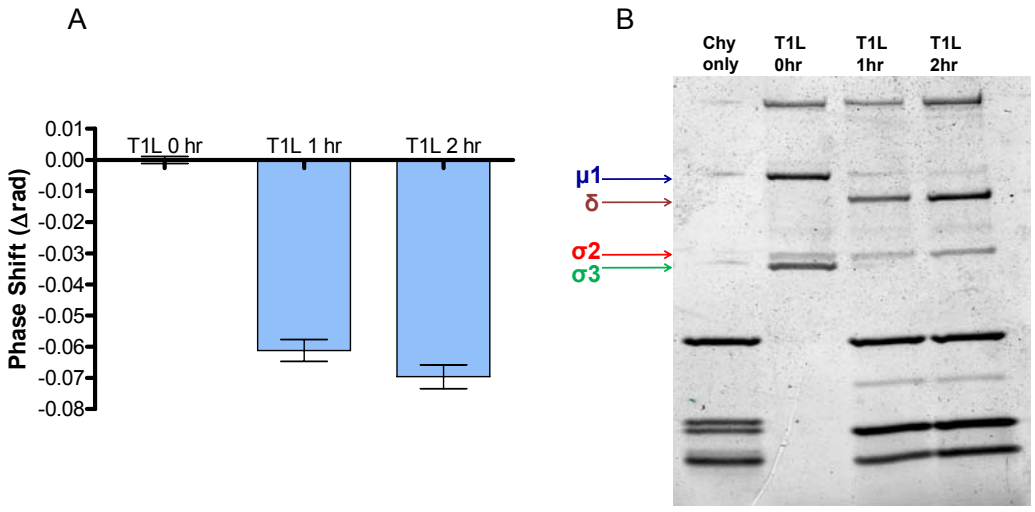

Figure 4.4 Chymotrypsin digest of reovirus T1L strain as evidenced by A) comparison of the BSI signal of T1L products before and after exposure to chymotrypsin (error bars represent 3 trials) and B) SDS-Page gel of these same products. *Note: SDS-PAGE gel performed by Joshua Doyle (Dermody lab).*

Conclusions

Although these experiments are in the preliminary stages, the results help bolster the suspicion that the source of the BSI signal is related to conformational changes in molecules. In particular, the detection of a marked difference between virion and ISVP (and between these stages and a more complete conversion to ISVP) suggests that BSI can detect viral degradation/conversion. These findings may enable the harnessing of induced conformational changes for optimized label-free signaling in diagnostic assays; specifically, environmental conditions such as pH, ionic strength, and/or the presence of proteases may be used strategically to determine unique profiles for specific analytes, such as a particular virus strain. Furthermore, molecules which generate a significant BSI signal in response to these conditions may be attached to probes as signaling

moieties, serving to enhance the BSI measurement of more elusive analytes that do not produce large conformational changes on their own.

In addition to the potential implications for BSI biosensing, these findings also imply the possibility that a low pH alone may have a role in the conformational changes occurring upon reovirus entry into the cell, rather than serving strictly to provide a functional environment for acid-dependent proteases (Figure 4.3). However, more studies are necessary to support this theory. Perhaps more importantly, Figure 4.4 shows that BSI may be a valuable tool for aiding in the characterization of reovirus conversion kinetics, and potential experiments comparing different reovirus strains and mutants may lend insight into important kinetic differences in the proteolytic disassembly of these species.

CHAPTER V

SYNOPSIS AND CONCLUSIONS

As shown in Chapters I and II, interferometry continues to be a powerful approach to biosensing. While each method discussed or reported elsewhere has advantages, it appears that BSI is somewhat unique, enabling previously impossible molecular interactions studies. In particular, BSI enables both free-solution and surface-immobilized assay formats, allowing for enormous flexibility in quantifying binding affinities, determining labeling perturbations, screening for binding, and detecting the presence of analytes in diagnostic applications.

The potential application of BSI as a diagnostic tool is demonstrated in Chapter III, highlighting that BSI can detect relevant antibody analytes against a background of human serum using antigen probes. These results suggest that BSI may be used as a reactive serum detector for syphilis, HIV, and virtually any other disease causing a significant and specific immune response. Furthermore, the correlation of BSI signal with titer strength in nontreponemal syphilis serology assays using clinical samples demonstrates quantitative potential of BSI in diagnostic applications. While additional studies are necessary to evaluate the performance of BSI in a point-of-care setting, these preliminary studies and the knowledge that BSI is a simple, rapid optical method compatible with microfluidics show promise for clinical applications of this technique.

The source of the BSI signal is explored in Chapter IV in preliminary studies using reovirus as a model for measuring induced, specific conformational changes.

Results suggest that BSI does indeed measure conformational changes, even in the absence of binding, such as the conversion of reovirus virions into ISVP particles. As we continue efforts to better understand how these conformational changes contribute to the BSI signal, we aim to harness induced conformational changes to diagnostic and other applications. Furthermore, expounding upon these studies may provide valuable kinetic information regarding the mechanism of reovirus entry into cells, lending insight into processes which are common among many clinically relevant viral infections.

REFERENCES

(1) Herschel, W. *Philosophical Transactions of the Royal Society of London* **1805**, *95*, 31-64.

(2) Michelson, A. A.; Pease, F. G. *The Astrophysical Journal* **1921**, *53*, 249-259.

(3) Baldwin, J. E.; Haniff, C. A. *Philosophical Transactions: Mathematical, Physical and Engineering Sciences* **2002**, *360*, 969-986.

(4) van Deelen, W.; Nisenson, P. *Applied Optics* **1969**, *8*, 951-&.

(5) Bruning, J. H.; Herriott, D. R.; Gallaghe.Je; Rosenfel.Dp; White, A. D.; Brangacc.Dj *Applied Optics* **1974**, *13*, 2693-2703.

(6) Scudieri, F. *Applied Optics* **1980**, *19*, 404-408.

(7) Goldstein, R. M.; Zebker, H. A. *Nature* **1987**, *328*, 707-709.

(8) Graber, H. C.; Thompson, D. R.; Carande, R. E. *Journal of Geophysical Research-Oceans* **1996**, *101*, 25813-25832.

(9) Vincent, P.; Larsen, S.; Galloway, D.; Laczniak, R. J.; Walter, W. R.; Foxall, W.; Zucca, J. J. *Geophysical Research Letters* **2003**, *30*, -.

(10) Massonnet, D.; Rossi, M.; Carmona, C.; Adragna, F.; Peltzer, G.; Feigl, K.; Rabaute, T. *Nature* **1993**, *364*, 138-142.

(11) Fan, X. D.; White, I. M.; Shopoua, S. I.; Zhu, H. Y.; Suter, J. D.; Sun, Y. Z. *Analytica Chimica Acta* **2008**, *620*, 8-26.

(12) Brosinger, F.; Freimuth, H.; Lacher, M.; Ehrfeld, W.; Gedig, E.; Katerkamp, A.; Spener, F.; Cammann, K. *Sensors and Actuators B-Chemical* **1997**, *44*, 350-355.

(13) Prieto, F.; Sepulveda, B.; Calle, A.; Llobera, A.; Dominguez, C.; Abad, A.; Montoya, A.; Lechuga, L. M. *Nanotechnology* **2003**, *14*, 907-912.

(14) Prieto, F.; Sepulveda, B.; Calle, A.; Llobera, A.; Dominguez, C.; Lechuga, L. M. *Sensors and Actuators B-Chemical* **2003**, *92*, 151-158.

(15) Schipper, E. F.; Brugman, A. M.; Dominguez, C.; Lechuga, L. M.; Kooyman, R. P. H.; Greve, J. *Sensors and Actuators B-Chemical* **1997**, *40*, 147-153.

(16) Ymeti, A.; Kanger, J. S.; Greve, J.; Lambeck, P. V.; Wijn, R.; Heideman, R. G. *Applied Optics* **2003**, *42*, 5649-5660.

(17) Hradetzky, D.; Mueller, C.; Reinecke, H. *Journal of Optics a-Pure and Applied Optics* **2006**, *8*, S360-S364.

(18) Schmitt, K.; Schirmer, B.; Hoffmann, C.; Brandenburg, A.; Meyrueis, P. *Biosensors & Bioelectronics* **2007**, *22*, 2591-2597.

(19) Schneider, B. H.; Edwards, J. G.; Hartman, N. F. *Clinical Chemistry* **1997**, *43*, 1757-1763.

(20) Schneider, B. H.; Dickinson, E. L.; Vach, M. D.; Hoijer, J. V.; Howard, L. V. *Biosensors & Bioelectronics* **2000**, *15*, 13-22.

(21) Schneider, B. H.; Dickinson, E. L.; Vach, M. D.; Hoijer, J. V.; Howard, L. V. *Biosensors & Bioelectronics* **2000**, *15*, 597-604.

(22) St John, P. M.; Davis, R.; Cady, N.; Czajka, J.; Batt, C. A.; Craighead, H. G. *Analytical Chemistry* **1998**, *70*, 1108-1111.

(23) Goh, J. B.; Loo, R. W.; Goh, M. C. *Sensors and Actuators B-Chemical* **2005**, *106*, 243-248.

(24) Houle, J.; Kumaraswamy, S. *Nature Methods* **2007**, *4*, i-ii.

(25) Swann, M. J.; Peel, L. L.; Carrington, S.; Freeman, N. J. *Analytical Biochemistry* **2004**, *329*, 190-198.

(26) Lin, S. M.; Lee, C. K.; Lin, Y. H.; Lee, S. Y.; Sheu, B. C.; Tsai, J. C.; Hsu, S. M. *Biosensors & Bioelectronics* **2006**, *22*, 715-721.

(27) Ricard-Blum, S.; Peel, L. L.; Ruggiero, F.; Freeman, N. J. *Analytical Biochemistry* **2006**, *352*, 252-259.

(28) Wang, J.; Xu, X. W.; Zhang, Z. X.; Yang, F.; Yang, X. R. *Analytical Chemistry* **2009**, *81*, 4914-4921.

(29) Baird, C. L.; Myszka, D. G. *Journal of Molecular Recognition* **2001**, *14*, 261-268.

(30) www.farfield-group.com

(31) Lin, V. S. Y.; Motesharei, K.; Dancil, K. P. S.; Sailor, M. J.; Ghadiri, M. R. *Science* **1997**, *278*, 840-843.

(32) Dancil, K. P. S.; Greiner, D. P.; Sailor, M. J. *Journal of the American Chemical Society* **1999**, *121*, 7925-7930.

(33) Li, Y. Y.; Cunin, F.; Link, J. R.; Gao, T.; Betts, R. E.; Reiver, S. H.; Chin, V.; Bhatia, S. N.; Sailor, M. J. *Science* **2003**, *299*, 2045-2047.

(34) Varma, M. M.; Inerowicz, H. D.; Regnier, F. E.; Nolte, D. D. *Biosensors & Bioelectronics* **2004**, *19*, 1371-1376.

(35) Varma, M. M.; Nolte, D. D.; Inerowicz, H. D.; Regnier, F. E. *Optics Letters* **2004**, *29*, 950-952.

(36) Zhao, M.; Nolte, D.; Cho, W. R.; Regnier, F.; Varma, M.; Lawrence, G.; Pasqua, J. *Clinical Chemistry* **2006**, *52*, 2135-2140.

(37) Wang, X. F.; Zhao, M.; Nolte, D. D. *Analytical and Bioanalytical Chemistry* **2009**, *393*, 1151-1156.

(38) Ozkumur, E.; Needham, J. W.; Bergstein, D. A.; Gonzalez, R.; Cabodi, M.; Gershoni, J. M.; Goldberg, B. B.; Unlu, M. S. *Proceedings of the National Academy of Sciences of the United States of America* **2008**, *105*, 7988-7992.

(39) Özkumur, E.; Yalçin, A.; Cretich, M.; Lopez, C. A.; Bergstein, D. A.; Goldberg, B. B.; Chiari, M.; Ünlü, M. S. *Biosensors & Bioelectronics* **2009**, *25*, 167-172.

(40) Birkert, O.; Gauglitz, G. *Analytical and Bioanalytical Chemistry* **2002**, *372*, 141-147.

(41) Birkert, O.; Tunnernann, R.; Jung, G.; Gauglitz, G. *Analytical Chemistry* **2002**, *74*, 834-840.

(42) Qavi, A. J.; Washburn, A. L.; Byeon, J. Y.; Bailey, R. C. *Analytical and Bioanalytical Chemistry* **2009**, *394*, 121-135.

(43) www.biametrics.com.

(44) Bornhop, D. J. *Applied Optics* **1995**, *34*, 3234-3239.

(45) Markov, D. A.; Bornhop, D. J. *Fresenius Journal of Analytical Chemistry* **2001**, *371*, 234-237.

(46) Swinney, K.; Bornhop, D. J. *Electrophoresis* **2001**, *22*, 2032-2036.

(47) Swinney, K.; Bornhop, D. J. *Electrophoresis* **2002**, *23*, 613-620.

(48) Sorensen, H. S.; Pranov, H.; Larsen, N. B.; Bornhop, D. J.; Andersen, P. E. *Analytical Chemistry* **2003**, *75*, 1946-1953.

(49) Wang, Z. L.; Swinney, K.; Bornhop, D. J. *Electrophoresis* **2003**, *24*, 865-873.

(50) Markov, D. A.; Dotson, S.; Wood, S.; Bornhop, D. J. *Electrophoresis* **2004**, *25*, 3805-3809.

(51) Wang, Z. L.; Bornhop, D. J. *Analytical Chemistry* **2005**, *77*, 7872-7877.

(52) Markov, D.; Begari, D.; Bornhop, D. J. *Analytical Chemistry* **2002**, *74*, 5438-5441.

(53) Markov, D. A.; Swinney, K.; Bornhop, D. J. *Journal of the American Chemical Society* **2004**, *126*, 16659-16664.

(54) Latham, J. C.; Markov, D. A.; Sorensen, H. S.; Bornhop, D. J. *Angewandte Chemie-International Edition* **2006**, *45*, 955-958.

(55) Englebienne, P.; Van Hoonacker, A.; Verhas, M. *Spectroscopy-an International Journal* **2003**, *17*, 255-273.

(56) Bornhop, D. J.; Latham, J. C.; Kussrow, A.; Markov, D. A.; Jones, R. D.; Sorensen, H. S. *Science* **2007**, *317*, 1732-1736.

(57) Kussrow, A.; Kaltgrad, E.; Wolfenden, M. L.; Cloninger, M. J.; Finn, M. G.; Bornhop, D. J. *Analytical Chemistry* **2009**, *81*, 4889-4987.

(58) Taguchi, T.; Takeyama, H.; Matsunaga, T. *Biosensors & Bioelectronics* **2005**, *20*, 2276-2282.

(59) Latham, J. C.; Stein, R. A.; Bornhop, D. J.; Mchaourab, H. S. *Analytical Chemistry* **2009**, *81*, 1865-1871.

(60) Bucciantini, M.; Giannoni, E.; Chiti, F.; Baroni, F.; Formigli, L.; Zurdo, J. S.; Taddei, N.; Ramponi, G.; Dobson, C. M.; Stefani, M. *Nature* **2002**, *416*, 507-511.

(61) Forman, M. S.; Lee, V. M. Y.; Trojanowski, J. Q. *Trends in Neurosciences* **2003**, *26*, 407-410.

(62) Polifke, T.; Rauch, P. *Genetic Engineering & Biotechnology News* **2008**, *28*, 43-45.

(63) Domeika, M.; Litvinenko, I.; Smirnova, T.; Gaivaronskaya, O.; Savicheva, A.; Sokolovskiy, E.; Ballard, R. C.; Unemo, M. *Journal of the European Academy of Dermatology and Venereology* **2008**, *22*, 1094-1100.

(64) Larsen, S. A.; Pope, V.; Johnson, R. E.; Edward J. Kennedy, J., Eds. *A Manual of the Tests for Syphilis*, 9th ed.; American Public Health Association: Washington DC, 1998.

(65) Kent, M. E.; Romanelli, F. *Annals of Pharmacotherapy* **2008**, *42*, 226-236.

(66) Golden, M. R.; Marra, C. M.; Holmes, K. K. *Jama-Journal of the American Medical Association* **2003**, *290*, 1510-1514.

(67) Tang, J. W.; Wong, B. C. K.; Lam, E.; Tai, V.; Lee, N.; Cockram, C. S.; Chan, P. K. S. *Journal of Medical Virology* **2008**, *80*, 1515-1522.

(68) Bhardwaj, D.; Bhatt, S.; Khamar, B. M.; Modi, R. I.; Ghosh, P. K. *Current Science* **2006**, *91*, 913-917.

(69) Iweala, O. I. *Contraception* **2004**, *70*, 141-147.

(70) Li, C. C.; Seidel, K. D.; Coombs, R. W.; Frenkel, L. M. *Journal of Clinical Microbiology* **2005**, *43*, 3901-3905.

(71) Erikstrup, C.; Kallestrup, P.; Zinyama-Gutsire, R. B. L.; Gomo, E.; Luneborg-Nielsen, M.; Gerstoft, J.; Schupbach, J.; Ullum, H.; Katzenstein, T. L. *Jaids-Journal of Acquired Immune Deficiency Syndromes* **2008**, *48*, 345-349.

(72) Project, E.; Friedman, R.; Nachliel, E.; Gutman, M. *Biophysical Journal* **2006**, *90*, 3842-3850.

(73) Yap, T. A.; Brunetto, A.; Pandha, H.; Harrington, K.; de Bono, J. S. *Expert Opinion on Investigational Drugs* **2008**, *17*, 1925-1935.

(74) Kelly, K.; Nawrocki, S.; Mita, A.; Coffey, M.; Giles, F. J.; Mita, M. *Expert Opinion on Biological Therapy* **2009**, *9*, 817-830.

(75) Hadzisejdic, I.; Cheng, K. D.; Wilkins, J. A.; Ens, W.; Coombs, K. M. *Rapid Communications in Mass Spectrometry* **2006**, *20*, 438-446.

(76) Alain, T.; Kim, T. S. Y.; Lun, X. Q.; Liacini, A.; Schiff, L. A.; Senger, D. L.; Forsyth, P. A. *Molecular Therapy* **2007**, *15*, 1512-1521.

(77) Coombs, K. M. *Virology* **1998**, *243*, 218-228.

(78) Nibert, M. L.; Chappell, J. D.; Dermody, T. S. *Journal of Virology* **1995**, *69*, 5057-5067.

(79) Golden, J. W.; Bahe, J. A.; Lucas, W. T.; Nibert, M. L.; Schiff, L. A. *Journal of Biological Chemistry* **2004**, *279*, 8547-8557.